EXPLORING SPHERICAL IMAGES PROPERTIES FROM OFF-THE-SHELF CAMERAS

Inácio Fonseca, MSc Student
I.S.R.-Institute of Systems and Robotics, Electrical Engineering Department,
University of Coimbra, Pinhal de Marrocos, 3030 - COIMBRA, Portugal
e-mail: sousa@isr.uc.pt

Jorge Dias, PhD
I.S.R.-Institute of Systems and Robotics, Electrical Engineering Department,
University of Coimbra, Pinhal de Marrocos, 3030 - COIMBRA, Portugal
e-mail: jorge@isr.uc.pt

ABSTRACT

This paper addresses the implementation of a mechatronic device to explore spherical image properties using off-the-shelf cameras. The article describes the improvements and extension performed on a first prototype built around mirrors, simulating the positioning of cameras in a spherical surface. This first prototype was tested as visual sensor of the navigation control module of a mobile robot, and this new mechatronic will be use to improve the vehicle's autonomy. The navigational process controls the steering and forward movements using visual information as feedback and using the images acquired in different positions in the sphere. The success of the first prototype version inspired us to improve the system for a new version, where new image sphere properties could be explored.

1 INTRODUCTION

This article presents ours efforts to develop a mechatronic device to explore spherical image properties, using off-the-shelf cameras. The first prototype developed is described, as well as its features and how the image sphere properties are explored. Based on this prototype, a set of experimental results are presented for an application for mobile robot navigation. In the last section we present a new mechatronic device, that improves the initial prototype and enables the exploration of other image sphere properties.

Several solutions have been proposed by different authors to drive a mobile robot indoors (see [5,6 and 7] for some examples), but here we propose a different solution, based on image sphere properties. In the next section we introduce a model for the image sphere, analyzing it mathematically.

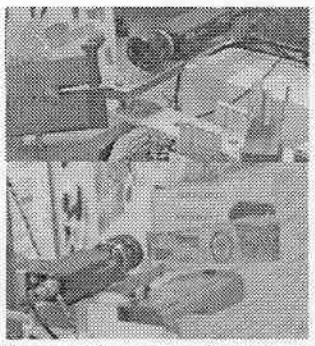

Figure 1. The actual system with the mirror setup to simulate four points of view in the sphere surface.

2 IMAGE SPHERE MODEL

Suppose that we want to control the attitude of a vehicle in the space, while the system is moving with translational velocity. Considering the referential system represented in the Fig. 2 and modeling the visual sensor as a spherical sensor with a radius r, we only need to control two rotational velocities indicated in the figure.

The first problem is how to determine the minimal number of cameras to use and where to

put them in the spherical surface to estimate the necessary information to control the vehicle. Bergholm [1] argues that the flow measured in the spherical equator perpendicular to the direction of translation, gives an estimation about the depth. To analyze the self-projected flow (ego-motion) in the spherical surface we will set $r=1$ by convenience but without losing generality.

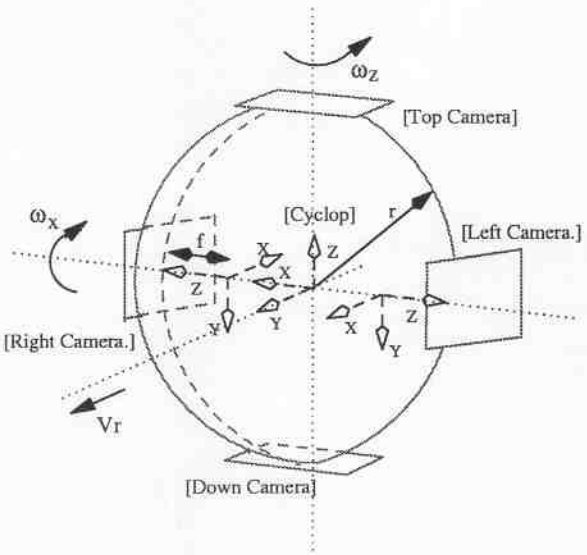

Figure 2:The sphere model for the navigation system in a three dimensional world.

The sphere's velocity can be described as $(\vec{v},\vec{\omega})$ with $\vec{v},\vec{\omega} \in R^3$. Let d be the distance from the sphere center to a three-dimensional point X with a vector $\vec{x}$ (the depth of the viewed point).

Then $d=\sqrt{x^2+y^2+z^2}$ and the following relation is valid:

$$\dot{\vec{x}} = \vec{\omega} \wedge \vec{x} + (\vec{v}/d)\cdot\|\vec{x}\| \qquad (1)$$

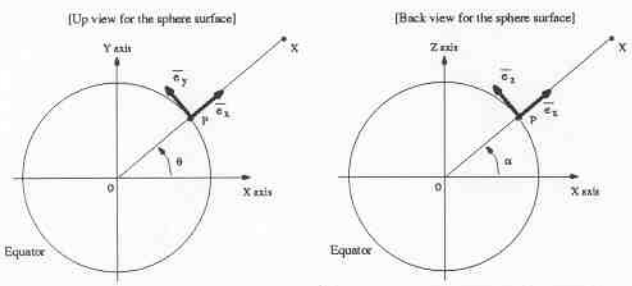

Figure 3: Decomposition of $\dot{\vec{p}}$ velocity in the referential described by the vectors $[\vec{e}_x,\vec{e}_y,\vec{e}_z]$.

It is also true, that any point P belonging to the X projection line can be described as $\vec{p}=\mu\cdot\vec{x},\mu>0$, and in particular if P belongs to the sphere surface then $\|\vec{p}\|=1$. The X velocity projected in the sphere point P is then given by :

$$\dot{\vec{p}} = \vec{\omega} \wedge \vec{p} + (\vec{v}/d)\cdot\|\vec{p}\| \qquad (2)$$

This velocity vector can be decomposed in any orthogonal referential, and in particular our choice will be the left referential represented in Fig. 3 by $[\vec{e}_x,\vec{e}_y,\vec{e}_z]$, because with this choice we can study the flow in the equator and in the direction normal to the equator. The point P described in referential $[\vec{e}_x,\vec{e}_y,\vec{e}_z]$ has coordinates $[\cos(\theta),\sin(\theta),0]$, the vectors are given by $\vec{e}_y=[-\sin(\theta),\cos(\theta),0]$, $\vec{e}_z=[0,0,1]$, and the $\vec{e}_x$ is not important because we cannot measure this flow in the sphere surface. In this case we will have:

$$\begin{cases} \vec{e}_y\cdot\dot{\vec{p}} = \omega_z + \cos(\theta)\cdot v_y/d - \sin(\theta)\cdot v_x/d \\ \vec{e}_z\cdot\dot{\vec{p}} = \omega_x\cdot\sin(\theta) - \omega_y\cdot\cos(\theta) + v_z/d \end{cases} \qquad (3)$$

However, in our case the sphere velocities are given by $\vec{v}=[0,v_y,\ 0]$ or $\vec{v}=[0,v_r,0]$ and $\vec{\omega}=[\omega_x,0,\omega_z]$ so the equation (3) reduces to:

$$\begin{cases} \vec{e}_y\cdot\dot{\vec{p}} = \omega_z + \cos(\theta)\cdot v_y/d \\ \vec{e}_z\cdot\dot{\vec{p}} = \omega_x\cdot\sin(\theta) \end{cases} \qquad (4)$$

That is, with the equator normal flow $\vec{e}_z\cdot\dot{\vec{p}}$ we can estimate the ω_x velocity because it not depends from depth d. The equator parallel flow $\vec{e}_y\cdot\dot{\vec{p}}$ depends from ω_z but using the difference between the optical flow sensed in two points it is possible to remove it. Notice that the study described earlier, can be also done for the plane $y=0$ and after doing the same analysis for the equator normal flow now $\vec{e}_y\cdot\dot{\vec{p}}$ and equator parallel flow now $\vec{e}_z\cdot\dot{\vec{p}}$ (now using the right referential in Fig. 3 by $[\vec{e}_x,\vec{e}_y,\vec{e}_z]$):

$$\begin{cases} \vec{e}_y\cdot\dot{\vec{p}} = \cos(\alpha)\cdot\omega_z - \sin(\alpha)\cdot\omega_x + v_y/d \\ \vec{e}_z\cdot\dot{\vec{p}} = 0 \end{cases} \qquad (5)$$

From this analytic study we conclude that using

the velocity measured in the sphere can be used to control the system. In fact comparing the optical flow from different points in the sphere is equivalent to compare the depth between two (or more) three dimensional points in space. This is the when we compare divergent points in the sphere.

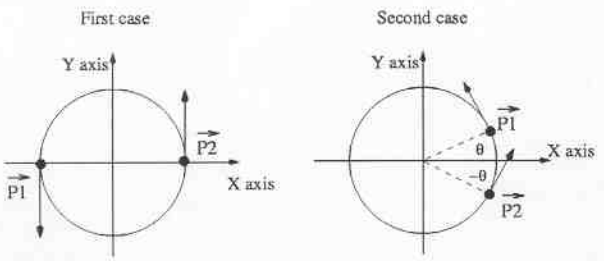

Figure 4: Representation of the relevant points to control the ω_z velocity.

For simplicity let's first consider the ω_z control. Looking for the Fig 4, We have for the first case with divergent points, where the flow $\vec{e}_y \cdot \dot{\vec{p}}$ is used (equation 4),

- $\vec{e}_y \cdot \dot{\vec{p}}_2 + \vec{e}_y \cdot \dot{\vec{p}}_1 = 2\omega_z + v_y\left(\frac{1}{d_2} - \frac{1}{d_1}\right)$ that depends from ω_z
- $\vec{e}_y \cdot \dot{\vec{p}}_2 - \vec{e}_y \cdot \dot{\vec{p}}_1 = v_y\left(\frac{1}{d_1} + \frac{1}{d_2}\right)$ and we can not compute the depth between the two points

Looking now for the second case in the same Fig. and using two points of view from the same lateral position, where the flow $\vec{e}_y \cdot \dot{\vec{p}}$ is used (equation 4),

- $\vec{e}_y \cdot \dot{\vec{p}}_2 + \vec{e}_y \cdot \dot{\vec{p}}_1 = 2\omega_z + 2\cos(\theta)v_y\left(\frac{1}{d_2} + \frac{1}{d_1}\right)$ - that depends from ω_z
- $\vec{e}_y \cdot \dot{\vec{p}}_2 - \vec{e}_y \cdot \dot{\vec{p}}_1 = \cos(\theta)v_y\left(\frac{1}{d_2} - \frac{1}{d_1}\right)$, it is possible to compare the depth between both points in presence of rotational movements ω_z and ω_x

From this analysis, the conclusion is that to control the ω_z velocity we must use four cameras, two for each lateral side. The control is also done in an independent way, i.e., we have a measure proportional to the orientation of each wall with the locomotion referential. For the control of ω_x we only need two cameras pointing as represented in Fig 2 by [Top Camera] and [Down Camera], because the ω_x value can be estimated by the flow given in the lateral cameras as explained earlier. So in this case using the equator normal flow $\vec{e}_y \cdot \dot{\vec{p}}$ from equation 5, the difference between the flow in the top and in the down side of the sphere is given by:

$$-2\omega_x + v_y\left(\frac{1}{d_1} - \frac{1}{d2}\right) \qquad (6)$$

where ω_x can be removed by using the estimation given by the equator normal flow $\vec{e}_z \cdot \dot{\vec{p}}$ of the equation 4.

Notice that if we chose to measure the feedback signal only when the mobile robot is moving with linear velocity, the system only needs to have the four cameras and the best positions are those represented in the Fig. 2. With the left and right cameras the system can sense and control the ω_z velocity and with the others two the ω_x velocity. However with only four cameras it is impossible to control the system while doing angular movements, and to solve this problem it will be used two points of view for each lateral camera as explained earlier.

2.1 Cameras Simulate a Spherical Sensor

In practice, we could use off-the-shelf cameras geometrically configured that acquire images corresponding to an image patch in the image sphere. To support the use of this principle we study this approach.

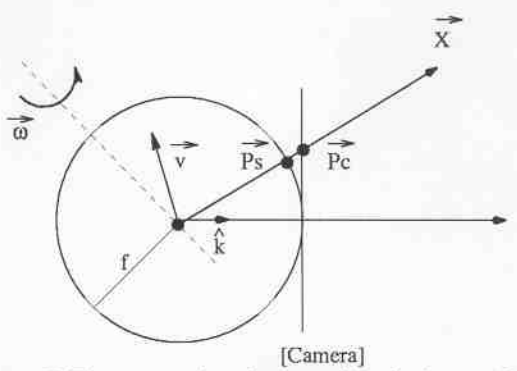

Figure 5: The conventional camera has the image plane tangent to a virtual spherical image sensor.

Considering the setup in Fig 5, the $\vec{x}$ velocity in the sphere point $\vec{p}_s$ is $\dot{\vec{p}}_s = \frac{\dot{\vec{x}}}{\|\vec{x}\|} f$, but we can

only measure in the sphere's surface the velocity $\dot{\vec{p}}_s = \frac{\dot{\vec{x}}}{\|\vec{x}\|} f - \frac{\dot{\vec{x}} \cdot \vec{x}}{\|\vec{x}\|^2} f \frac{\vec{x}}{\|\vec{x}\|}$. For the camera, differentiating the geometrical projection law $\vec{p}_c = \frac{f}{\vec{x} \cdot \hat{k}} \vec{x}$ in order of t, we can express $\dot{\vec{p}}_c = \frac{f}{\vec{x} \cdot \hat{k}} \dot{\vec{x}} - \frac{f}{(\vec{x} \cdot \hat{k})^2} (\dot{\vec{x}} \cdot \hat{k}) \vec{x}$, and using the $\vec{x}$ velocity in this expression, we will get the final result that unfortunately is not equal to the measured velocity in the sphere's surface. However if the $\vec{x}$ vector points in the $\hat{k}$ direction the two velocities are actually the same. So in conclusion, we can only use the portion of the digital image that is tangent with the spherical surface, because just at this position the measured velocities will be very similar.

3 ALGORITHM AND RESULTS

3.1 Control Algorithm

In this section it will be described the experimental system used to test the approach proposed in last section. A controller based on the signals given by four images is designed to control the steering of a mobile platform. In this experimental system the mirrors are positioned in stereo divergent way, simulating the acquisition of images in the image sphere's equator. To help the control and acquisition timings we use a DES (Discrete Event System) to monitor the algorithm presented in Fig 6. One of the states is responsible to monitor the acquisition and the other to monitor the communications with the mobile robot. Because the timings involved are different the final measure for each image is the mean in the acquisition interval.

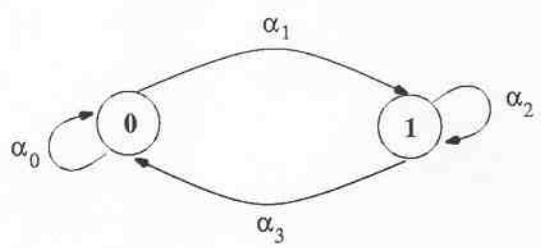

$\Sigma_u = \{ \alpha_0 , \alpha_1 , \alpha_2 , \alpha_3 \}$

Figure 6: The Discrete Event System definition. The states definitions are respectively: (State 0 – Acquisition, State 1 – Control)

The event description is:

- α0 - wait until the next control timing arrives, i.e., 0,5s doing measures
- α1 - acquisition finished
- α2 - control update not finished yet
- α3 - command sent successful for the robot

For steering control we use the lateral cameras, and two mirrors by camera. The signals generated from optical flow obtained from the images, give a direct estimation the vehicle's attitude relative to the lateral planes.

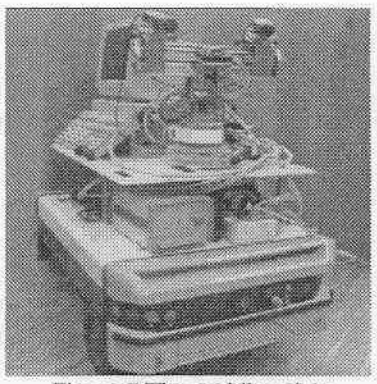

Figure 7:The mobile robot.

The signal measured in each image is the horizontal optical flow or as wish the horizontal displacement, that can be given by any one-dimensional optical flow or a correlation technique. In our case the both are used to give a strong validation for the measure. The mirror setup is represented in Fig. 8.

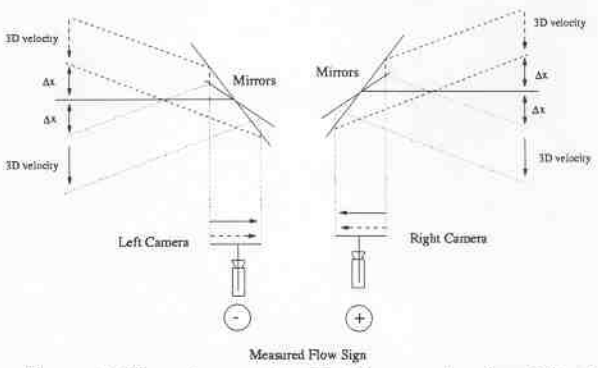

Figure 8: The mirror setup. In this case for simplicity the cameras do not have been represented as a geometrical model.

Considering the Fig. 8 and indicating the signals measured by:

- **FRMM** - Front Right Mirror Measure, optical flow measured in the front right image
- **BRMM** - Back Right Mirror Measure, optical flow

measured in the back right image

- **FLMM** - Front Right Mirror Measure, optical flow measured in the front left image
- **BLMM** - Back Right Mirror Measure, optical flow measured in the back left image

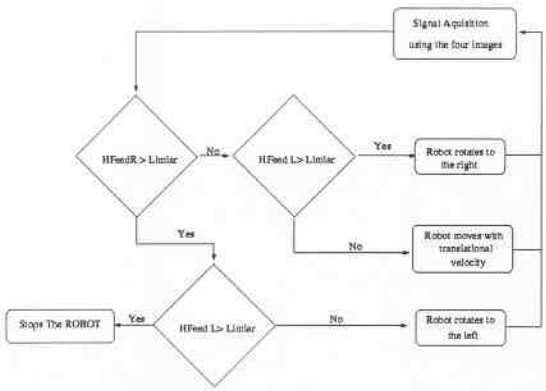

Figure 9: The control Algorithm diagram.

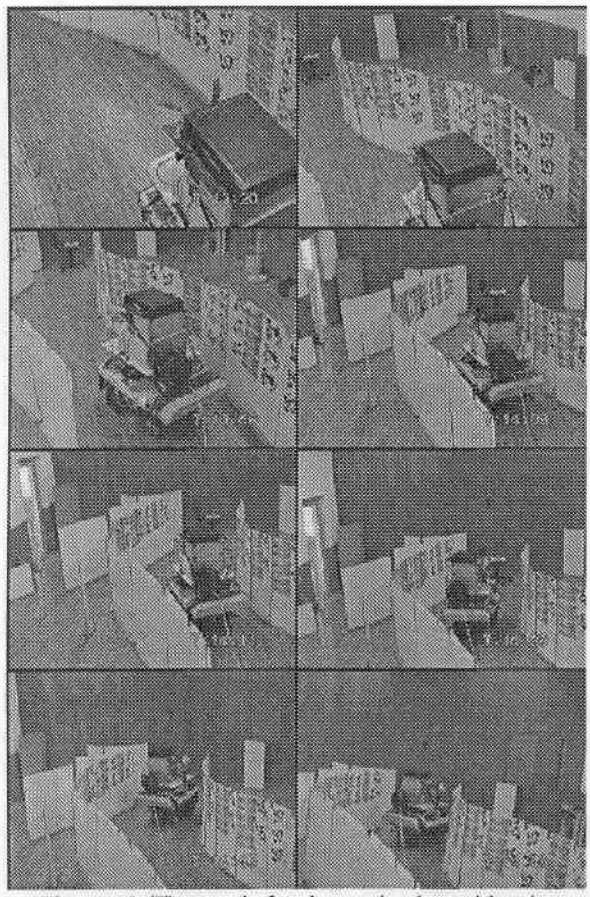

Figure 10: The result for the navigation with mirrors (external images).

The control strategy can be described as (just considering the right side):

- if $\|FRMM - BRMM\| <$ threshold then the robot can rotate to the left or do translations,
- if $FRMM - BRMM >$ threshold then the robot must rotate to the left,
- if $FRMM - BRMM <$ threshold then the robot can rotate to the left/right or going to the front (depends from the measures in the left side)

Defining *HfeedR* = *FRMM-BRMM* and *HfeedL* = *FLMM-BLMM* the algorithm including both sides can be described by the diagram represented in Fig. 9. In this case the forward velocity is constant and the system only controls the angular velocity. The acquisition loop timing is different from the control loop timing, in this case respectively 0.08 seconds and 0,5 seconds.

3.2 Experimental Results

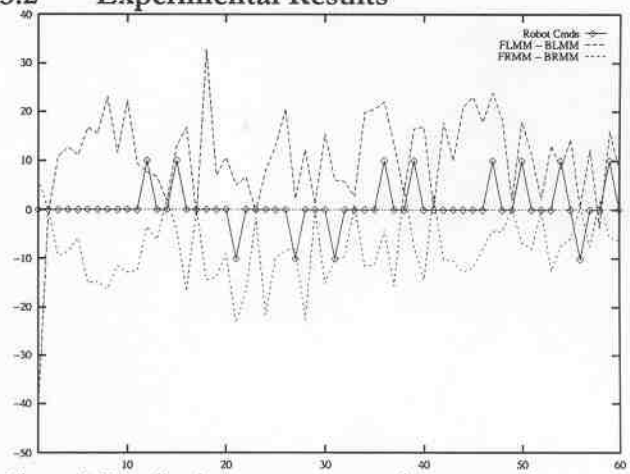

Figure 11:Feedback measures versus the commands sent to the mobile platform for the example showed in Fig 10. Time unit: 0,5 seconds. Commands: 0 - Forward movement, 10 - Right movement, 10 - Left movement.

The Figs. 10 shows the experimental results for the navigation process with mirrors and Fig 11 shows the measured signals to control the mobile platform.

4. SPHERICAL IMAGE SIMULATOR

The prototype that we plan to build in the future is represented in Fig 12,13 and 14. In this prototype, using a rotating mirror system and a rotating basis we simulate partially a small sphere's piece as showed in Fig. 13. In the construction we plan to use a camera pointing to the sky where is a mirror system similar to the one developed in the present work. The mirror system has two mirrors, one shows the left side and the other the right side. However each one can be moved by a motor that rotates it by using a two couple mechanical circles. The mirror system can be approximated to the camera by using the top motor. This is just do adjust the distance between the cameras and the mirrors (off-line procedure).

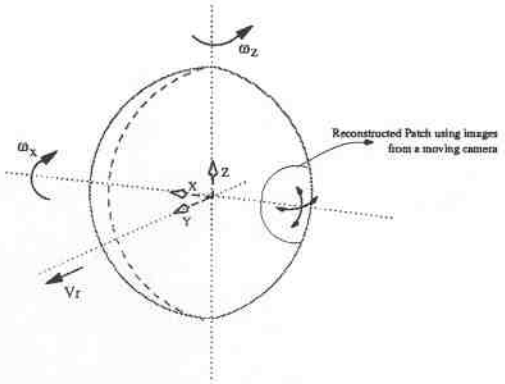

Figure 12: With the new prototype using a rotating basis and a rotating mirror system, we can cover the small circle represented.

The basis can rotate and all the system rotates with it, including the camera. Comparing this prototype to the previous, we have few cameras, but a more complex mechanical system. At this moment we have not yet any idea about the size, we hope that the small piece that supports the mirror system can also support the two small motors that change the two mirror's orientation.

5. CONCLUSIONS

The paper addressed the problem of visual based navigation, using a mobile robot. The vision system realizes partially the concept of image sphere by using a stereo divergent system. To obtain more than two images in the sphere, mirrors were used. The success obtained in the first prototype inspired us to continue with the philosophy of getting more accurate in the spherical sensor simulation.

REFERENCES

[1] F. Bergholm, "Decomposition Theory and Transformations of Visual Directions", ICCV 90- Int. Conf. on Computer Vision, Dec 1990, pp. 85-90.

[2] J. Dias, C. Paredes, I. Fonseca, H. Araújo,J. Batista, A.de Almeida, "Simulating pursuit with Machines - Experiments with Robots and Artificial Vision", ICRA'94, Int. Conference on Robotics and Automation,Nagoya, Japan, May 21-27, 1995.

[3] Jorge Dias, Carlos Paredes, Inácio Fonseca, Jorge Batista, Helder Araújo, A.de Almeida, " Simulating Pursuit with Machines, Using Active Vision and Mobile Robots", IEEE Transactions on Robotics and Automation, [in publication].

[4] Roger, A. S. and Schwartz, E.L. "Design considerations for a Space-Variant Sensor with Complex Logarithmic Geometry", Proc. 10th International Conference on Pattern Recognition,Atlantic City, pp. 278-285,1990.

[5]Alberto Elfes, " Robot Navigation: Integrating Perception, Environmental Constraints and Task Execution Within a Probabilistic Framework", International Workshop, Ressoning with Uncertainty in Robotics Conf. - RUR, 95, Amsterdam, The Netherlands, December 1995, Springer ISBN 3-540-61376-5.Proc.

[6] Andrew J Davison and David W Murray, "Mobile Robot Localisation Using Active Vision", Parks Road, Oxford University, 1997.

[7] D. Coombs, M. Herman, T. Hong and M. Nashman, " Real-time Obstacle Avoidance Using Central Flow Divergence and Peripheral Flow ", National Institute of Standards and Technology, Nist Internal Report, June, 1995.

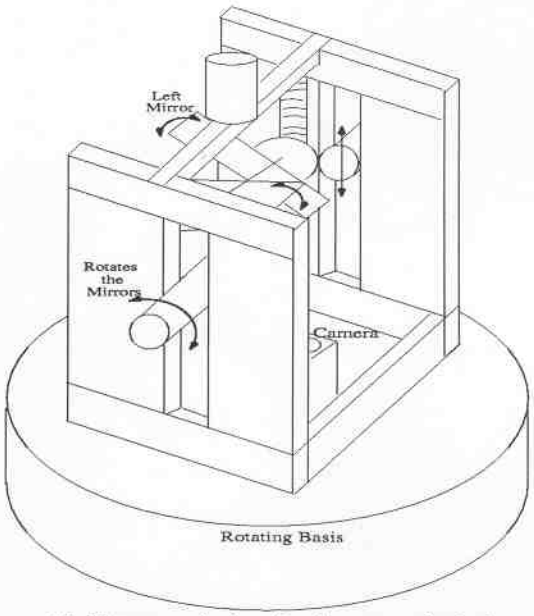

Figure 13: The general view for the new spherical sensor.

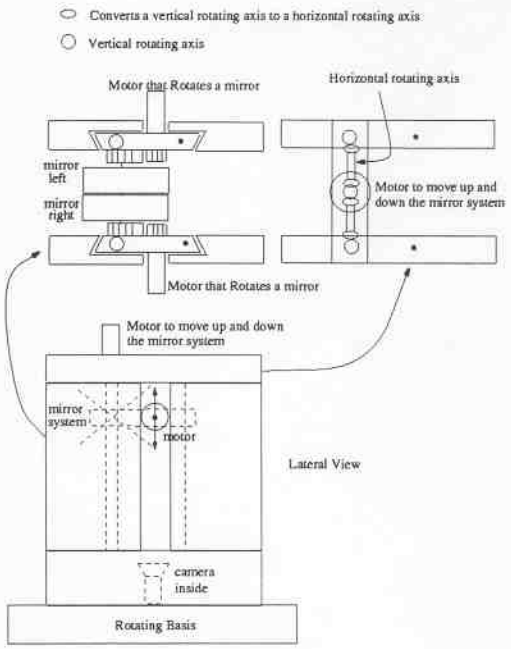

Figure 14: The prototype to the new spherical sensor simulation. This prototype uses a rotating basis (±90°) with only one camera, and a mirror system that can be rotated.